



Electron transport analysis in water vapor

Satoru Kawaguchi¹, Kazuhiro Takahashi², Kohki Satoh^{2*}, and Hidenori Itoh²

¹Division of Engineering, Graduate School of Muroran Institute of Technology, Muroran, Hokkaido 050-8585, Japan

²Division of Information and Electronic Engineering, Graduate School of Muroran Institute of Technology, Muroran, Hokkaido 050-8585, Japan

*E-mail: ksato@mmm.muroran-it.ac.jp

Received November 30, 2015; revised January 21, 2016; accepted January 30, 2016; published online xxxx yy, zzzz

A reliable set of electron collision cross sections for water vapor, including elastic, rotational, vibrational, and electronic excitation, electron attachment, and ionization cross sections, is estimated by the electron swarm method. In addition, anisotropic electron scattering for elastic and rotational excitation collisions is considered in the cross section set. Electron transport coefficients such as electron drift velocity, longitudinal diffusion coefficient, and effective ionization coefficient are calculated from the cross section set by Monte Carlo simulation in a wide range of E/N values, where E and N are the applied electric field and the number density of H_2O molecules, respectively. The calculated transport coefficients are in good agreement with those measured. The obtained results confirm that the anisotropic electron scattering is important for the calculation at low E/N values. Furthermore, the cross section set assuming the isotropic electron scattering is proposed for practical use.

© 2016 The Japan Society of Applied Physics

1. Introduction

Discharge plasma, generated in gases containing water vapor or generated in contact with liquid, has extensive applications, such as the promotion of plant growth,¹⁾ the disinfection of microorganisms,²⁻⁴⁾ and the decomposition of nondegradable hazardous substances.^{5,6)} Reactive nitrogen species (RNS), such as NO_3^- , and reactive oxygen species (ROS), such as H_2O_2 , are found to play important roles in these applications; thus, an appropriate method of controlling the concentrations of these species is needed to improve the efficiency of the applications. Plasma simulation is known as an effective tool for predicting the behavior of active species in plasmas, and such simulation has been carried out.⁷⁻⁹⁾

The reliability of plasma simulation coupled with rate equation analysis for chemical reaction processes depends on that of transport coefficients, such as a drift velocity and diffusion coefficient, and rate coefficients for species. In particular, electrons have high mobility and reactivity, so that accurate transport coefficients and rate coefficients for electrons are needed to improve the accuracy of plasma simulation. The transport coefficients for electrons are not only measured but also calculated from a set of electron collision cross sections by Monte Carlo simulation and Boltzmann equation analysis. Furthermore, measured transport coefficients are limited, so the calculation of transport coefficients from an accurate cross section set is important; therefore, an accurate cross section set is required.

Some cross section sets for water vapor have been reported.¹⁰⁻¹²⁾ Itikawa and Mason¹⁰⁾ reviewed measured and theoretically calculated electron collision cross sections for water vapor, and recommended a set of cross sections including momentum transfer, rotational, vibrational, and electronic excitation, electron attachment, and ionization cross sections, but they did not calculate the electron transport coefficients from their cross section set; therefore, the validity of the cross section set is not confirmed. Yousfi and Benabdessadok¹¹⁾ and de Urquijo et al.¹²⁾ estimated the cross section set for water vapor by the electron swarm method with Boltzmann equation analysis. In the calculation of the transport coefficients, the effect of superelastic collision for rotationally excited molecules is considered by Yousfi and Benabdessadok,¹¹⁾ and the effect of the

superelastic collision and anisotropic electron scattering for elastic and rotational excitation collisions are considered by de Urquijo et al.,¹²⁾ however, the electron drift velocity, longitudinal diffusion coefficient, and effective ionization coefficient calculated from the cross section sets in Refs. 11 and 12 do not necessarily agree with measured data in a wide range of E/N values, where E and N are the applied electric field and the number density of H_2O molecules, respectively.

In this work, we estimated the reliable cross section set for water vapor considering the anisotropic electron scattering for elastic and rotational excitation collisions. The electron transport coefficients such as the electron drift velocity, longitudinal diffusion coefficient, and effective ionization coefficient are calculated from the estimated cross section set by Monte Carlo simulation. Then, the validity of the estimated cross section set is confirmed by the comparison between calculated and measured transport coefficients. Furthermore, a set of electron collision cross sections for water vapor assuming isotropic electron scattering after elastic and rotational excitation collisions is estimated for practical use.

2. Electron collision cross sections (anisotropic scattering model)

Figure 1 shows the electron collision cross section set for water vapor estimated in this work. This cross section set consists of two vibrational excitations, three electron attachments, 26 electronic excitations, six ionizations, three rotational excitation cross sections, and one elastic collision cross section. Electron-molecule reactions considered here are listed in Table I. Symbol Σq_{ex} in Fig. 1 denotes the sum of electronic excitation cross sections, and the detailed cross sections for the electronic excitation are plotted in Fig. 2. The vibrational excitation cross sections follow experimental data obtained by Seng and Linder.¹³⁾ For the electron attachment, partial cross sections for O^- and H^- measured by Rawat et al.¹⁴⁾ and that for OH^- measured by Melton¹⁵⁾ are used. For the electronic excitation, 25 out of 26 partial cross sections follow those measured by Thorn and co-workers,¹⁶⁻²⁰⁾ and a cross section, the threshold energy of which is 12.5 eV, is estimated to fit the calculated effective ionization coefficient to the measured data. The ionization cross section consists of five partial dissociative ionization cross sections such as OH^+ , H^+ , O^+ , H_2^+ , and O_2^+ and a

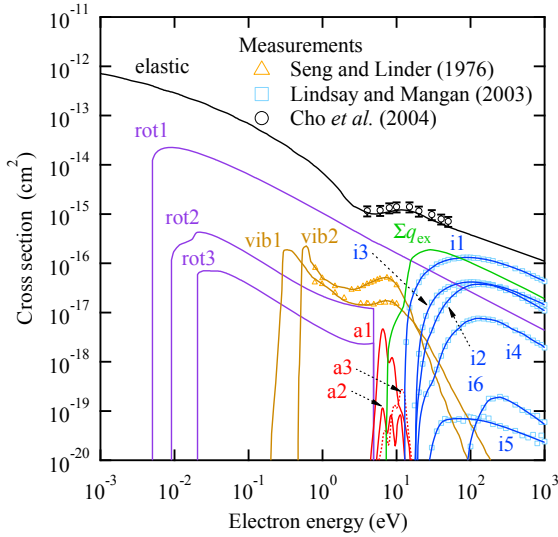


Fig. 1. (Color online) Electron collision cross sections of water vapor (anisotropic scattering model).

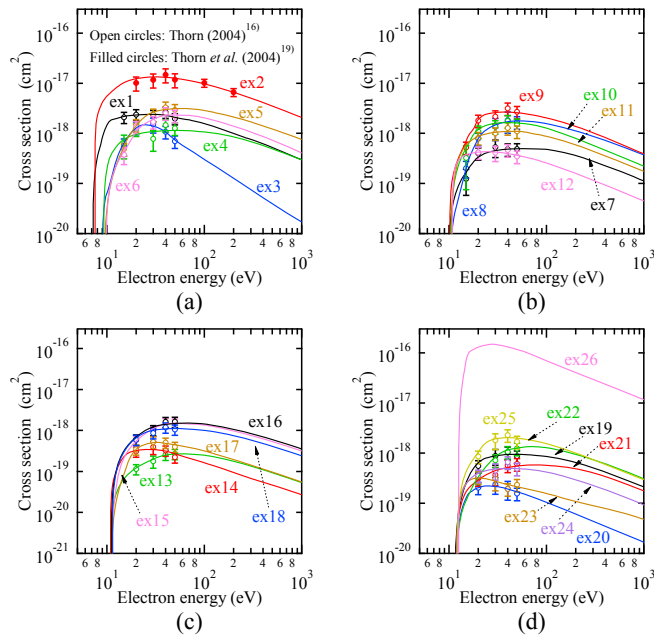


Fig. 2. (Color online) Electronic excitation cross sections: (a) ex1–ex6, (b) ex7–ex12, (c) ex13–ex18, and (d) ex19–ex26.

direct ionization cross section H_2O^+ , and those follow the data recalibrated by Lindsay and Mangan²¹⁾ using the measured data of Straub et al.²²⁾ The threshold energies of the ionization cross sections for H_2O^+ , OH^+ and H^+ , O^+ , and H_2^+ are obtained from the measured data by Snow and Thomas,²³⁾ Lefavre and Marmet,²⁴⁾ Morrison and Traeger,²⁵⁾ and Ehrhardt and Kresling²⁶⁾ listed in NIST Chemistry WebBook,²⁷⁾ respectively. The threshold energy of the cross section for O^{2+} is estimated as 80 eV by the extrapolation of the measured partial dissociative ionization cross section. Rotational excitation cross sections have been theoretically calculated owing to experimental difficulty. Itikawa and Mason¹⁰⁾ reported the rotational excitation cross sections for the transitions from $J=0$ to 1, 2, and 3 based on the data recently calculated by Faure et al.,²⁸⁾ where J is the rotational angular momentum. In this work, the recent and recom-

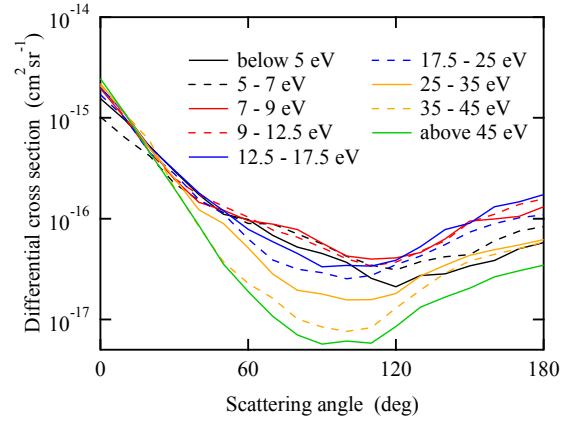


Fig. 3. (Color online) Differential cross sections for elastic and rotational excitation collisions.

mended cross sections by Itikawa and Mason are used, but multiplied by a factor of 0.1. The vibrationally elastic cross section, which is defined as the sum of the elastic and rotational excitation cross sections, is measured by Cho et al.,²⁹⁾ so that the elastic collision cross section is estimated from the data.

Figure 3 shows differential cross sections for elastic and rotational excitation collisions for different incident energies deduced from the data measured by Cho et al.²⁹⁾ The angular distributions are used after elastic and rotational excitation collisions.

3. Monte Carlo simulation

The behavior of electrons in free space under a uniform electric field $\mathbf{E} = (0, 0, -E)$ is traced by the Monte Carlo method, and electron transport coefficients such as the mean-arrival-time drift velocity W_m and longitudinal diffusion coefficient D_L for time-of-flight (TOF) sampling, the ionization coefficient α , electron attachment coefficient η , and effective ionization coefficient $\alpha - \eta$ for steady-state Townsend (SST) sampling are obtained. The definition and sampling principle of those transport coefficients are described in Refs. 30 and 31. The drift velocity W_m is related to the center-of-mass drift velocity W_r , which is also called the bulk drift velocity,³²⁾ and the relationship is described as³³⁾

$$W_m = W_r - 2(\alpha - \eta)D_L + 3(\alpha - \eta)^2D_3 - \dots, \quad (1)$$

where D_3 is the third-order diffusion coefficient in the field direction. The drift velocity W_m differs from the drift velocity W_r , and the electron drift velocity measured by the double-shutter drift tube method³⁴⁾ and pulsed experiment¹²⁾ should be compared with W_m .³⁵⁾ The calculation method of Monte Carlo simulation for electron behavior is described in Refs. 30 and 31.

The thermal motion of molecules and the anisotropic electron scattering are reported as important phenomena for the analysis of electron behavior in water vapor in a low E/N region. For the accurate simulation of electron behavior, the velocity \mathbf{v}' of an electron after a collision is calculated as³⁶⁾

$$\mathbf{v}' = \frac{M}{m+M}\mathbf{g}' + \frac{m\mathbf{v} + M\mathbf{V}}{m+M}, \quad (2)$$

where m and M are the masses of the electron and molecule, respectively, $\mathbf{V} = (V_x, V_y, V_z)$ and \mathbf{V}' are the velocities of the

Table I. Electron–water molecule reactions considered in the estimated cross section set.

Label	Type of collision	Reaction	ε_{th} (eV)	Ref.
mom ^{a)}	Momentum transfer ^{a)}	$\text{H}_2\text{O} + \text{e} \rightarrow \text{H}_2\text{O} + \text{e}$		29
rot1	Rotational excitation	$\text{H}_2\text{O} (J=0) + \text{e} \rightarrow \text{H}_2\text{O} (J=1) + \text{e}$	4.604×10^{-3}	10
rot2	Rotational excitation	$\text{H}_2\text{O} (J=0) + \text{e} \rightarrow \text{H}_2\text{O} (J=2) + \text{e}$	8.690×10^{-3}	10
rot3	Rotational excitation	$\text{H}_2\text{O} (J=0) + \text{e} \rightarrow \text{H}_2\text{O} (J=3) + \text{e}$	1.764×10^{-2}	10
vib1	Vibrational excitation	$\text{H}_2\text{O} (000) + \text{e} \rightarrow \text{H}_2\text{O} (010) + \text{e}$	0.198	13
vib2	Vibrational excitation	$\text{H}_2\text{O} (000) + \text{e} \rightarrow \text{H}_2\text{O} [(100) + (001)] + \text{e}$	0.466	13
a1	Electron attachment	$\text{H}_2\text{O} + \text{e} \rightarrow \text{H}^- + \text{OH}$	4.000	14
a2	Electron attachment	$\text{H}_2\text{O} + \text{e} \rightarrow \text{OH}^- + \text{H}$	4.016	15
a3	Electron attachment	$\text{H}_2\text{O} + \text{e} \rightarrow \text{O}^- + \text{H}_2$	4.300	14
ex1	Electronic excitation	$\text{H}_2\text{O} + \text{e} \rightarrow \text{H}_2\text{O}(\tilde{a}^3B_1) + \text{e}$	7.140	16–18
ex2	Electronic excitation	$\text{H}_2\text{O} + \text{e} \rightarrow \text{H}_2\text{O}(\tilde{A}^1B_1) + \text{e}$	7.490	19
ex3	Electronic excitation	$\text{H}_2\text{O} + \text{e} \rightarrow \text{H}_2\text{O}(\tilde{A}_2) + \text{e}$	8.900	16, 17
ex4	Electronic excitation	$\text{H}_2\text{O} + \text{e} \rightarrow \text{H}_2\text{O}(\tilde{A}_2) + \text{e}$	9.200	16, 17
ex5	Electronic excitation	$\text{H}_2\text{O} + \text{e} \rightarrow \text{H}_2\text{O}(\tilde{b}^3A_1) + \text{e}$	9.460	16–18
ex6	Electronic excitation	$\text{H}_2\text{O} + \text{e} \rightarrow \text{H}_2\text{O}(\tilde{B}^1A_1) + \text{e}$	9.730	16–18
ex7	Electronic excitation	$\text{H}_2\text{O} + \text{e} \rightarrow \text{H}_2\text{O}(\tilde{d}^3A_1) + \text{e}$	9.820	16, 20
ex8	Electronic excitation	$\text{H}_2\text{O} + \text{e} \rightarrow \text{H}_2\text{O}(\tilde{c}^3B_1 + \tilde{C}^1B_1) + \text{e}$	9.980	16, 20
ex9	Electronic excitation	$\text{H}_2\text{O} + \text{e} \rightarrow \text{H}_2\text{O}(\tilde{D}^1A_1) + \text{e}$	10.12	16, 20
ex10	Electronic excitation	$\text{H}_2\text{O} + \text{e} \rightarrow \text{H}_2\text{O}[\tilde{C}^1B_1(100) + \tilde{B}_1] + \text{e}$	10.35	16, 20
ex11	Electronic excitation	$\text{H}_2\text{O} + \text{e} \rightarrow \text{H}_2\text{O}[\tilde{B}_1 + \tilde{D}^1A_1(100)] + \text{e}$	10.55	16, 20
ex12	Electronic excitation	$\text{H}_2\text{O} + \text{e} \rightarrow \text{H}_2\text{O}(\tilde{A}_2) + \text{e}$	10.70	16, 20
ex13	Electronic excitation	$\text{H}_2\text{O} + \text{e} \rightarrow \text{H}_2\text{O}[\tilde{D}^1A_1(110) + \tilde{C}^1B_1(200)] + \text{e}$	10.77	16, 20
ex14	Electronic excitation	$\text{H}_2\text{O} + \text{e} \rightarrow \text{H}_2\text{O}(\tilde{A}_2) + \text{e}$	10.84	16, 20
ex15	Electronic excitation	$\text{H}_2\text{O} + \text{e} \rightarrow \text{H}_2\text{O}[\tilde{e}^3B_1 + \tilde{E}^1B_1 + \tilde{D}^1A_1(200)] + \text{e}$	10.97	16, 20
ex16	Electronic excitation	$\text{H}_2\text{O} + \text{e} \rightarrow \text{H}_2\text{O}(\tilde{B}_2 + \tilde{A}_2 + \tilde{B}_2) + \text{e}$	11.10	16, 20
ex17	Electronic excitation	$\text{H}_2\text{O} + \text{e} \rightarrow \text{H}_2\text{O}(\tilde{A}_1 + \tilde{A}_2 + \tilde{A}_1 + \tilde{A}_2 + \tilde{B}_1 + \tilde{B}_1) + \text{e}$	11.23	16, 20
ex18	Electronic excitation	$\text{H}_2\text{O} + \text{e} \rightarrow \text{H}_2\text{O}(\tilde{B}_1 + \tilde{B}_1 + \tilde{A}_1 + \tilde{A}_1) + \text{e}$	11.35	16, 20
ex19	Electronic excitation	$\text{H}_2\text{O} + \text{e} \rightarrow \text{H}_2\text{O}(\tilde{B}_2 + \tilde{B}_2 + \tilde{B}_1 + \tilde{B}_1) + \text{e}$	11.50	16, 20
ex20	Electronic excitation	$\text{H}_2\text{O} + \text{e} \rightarrow \text{H}_2\text{O}(\tilde{A}_2 + \tilde{A}_2) + \text{e}$	11.61	16, 20
ex21	Electronic excitation	$\text{H}_2\text{O} + \text{e} \rightarrow \text{H}_2\text{O}(\tilde{B}_1) + \text{e}$	11.68	16, 20
ex22	Electronic excitation	$\text{H}_2\text{O} + \text{e} \rightarrow \text{H}_2\text{O}(\tilde{B}_1) + \text{e}$	11.75	16, 20
ex23	Electronic excitation	$\text{H}_2\text{O} + \text{e} \rightarrow \text{H}_2\text{O}(\tilde{A}_1 + \tilde{A}_1) + \text{e}$	11.80	16, 20
ex24	Electronic excitation	$\text{H}_2\text{O} + \text{e} \rightarrow \text{H}_2\text{O}(\tilde{A}_1 + \tilde{B}_1 + \tilde{B}_1) + \text{e}$	11.90	16, 20
ex25	Electronic excitation	$\text{H}_2\text{O} + \text{e} \rightarrow \text{H}_2\text{O}(\tilde{A}_1) + \text{e}$	12.06	16, 20
ex26	Electronic excitation	$\text{H}_2\text{O} + \text{e} \rightarrow \text{H}_2\text{O}^* + \text{e}$	12.50	
i1	Ionization	$\text{H}_2\text{O} + \text{e} \rightarrow \text{H}_2\text{O}^+ + 2\text{e}$	12.65	21, 23
i2	Ionization	$\text{H}_2\text{O} + \text{e} \rightarrow \text{H}^+ + \text{OH} + 2\text{e}$	16.95	21, 24
i3	Ionization	$\text{H}_2\text{O} + \text{e} \rightarrow \text{OH}^+ + \text{H} + 2\text{e}$	18.08	21, 24
i4	Ionization	$\text{H}_2\text{O} + \text{e} \rightarrow \text{O}^+ + \text{H}_2 + 2\text{e}$	19.00	21, 25
i5	Ionization	$\text{H}_2\text{O} + \text{e} \rightarrow \text{H}_2^+ + \text{O} + 2\text{e}$	20.70	21, 26
i6	Ionization	$\text{H}_2\text{O} + \text{e} \rightarrow \text{O}^{2+} + \text{H}_2 + 3\text{e}$	80.00	21

a) Elastic.

molecule before and after the collision, respectively, \mathbf{v} is the velocity of the electron before the collision, and \mathbf{g}' is the relative velocity of the electron to the molecule after the collision described as $\mathbf{g}' = \mathbf{v}' - \mathbf{V}$. \mathbf{V} is calculated from the Maxwell–Boltzmann distribution with the gas temperature T_g using the Box–Muller method³⁷⁾ as

$$V_x = \sqrt{-2k_B T_g \log \xi_1 / M} \cos(2\pi\xi_2), \quad (3a)$$

$$V_y = \sqrt{-2k_B T_g \log \xi_1 / M} \sin(2\pi\xi_2), \quad (3b)$$

$$V_z = \sqrt{-2k_B T_g \log \xi_3 / M} \cos(2\pi\xi_4), \quad (3c)$$

where k_B is the Boltzmann constant and ξ is the random number uniformly distributed on $[0, 1]$. The relative velocity \mathbf{g}' is calculated as

$$\mathbf{g}' = |\mathbf{g}'| \begin{bmatrix} \cos \theta \cos \phi & -\sin \phi & \sin \theta \cos \phi \\ \cos \theta \sin \phi & \cos \phi & \sin \theta \sin \phi \\ -\sin \theta & 0 & \cos \theta \end{bmatrix} \times \begin{bmatrix} \sin \chi \cos \psi \\ \sin \chi \sin \psi \\ \cos \chi \end{bmatrix}, \quad (4)$$

where θ and ϕ are respectively the polar and azimuthal angles of the relative velocity $\mathbf{g} = \mathbf{v} - \mathbf{V}$ in a laboratory system, and the scattering angles χ and ψ are respectively the polar and azimuthal angles of \mathbf{g}' in the coordinate system where \mathbf{g} is directed along the z -axis as shown in Fig. 4.³⁸⁾ The scattering angle χ is obtained from Eq. (5), and ψ from Eq. (6),

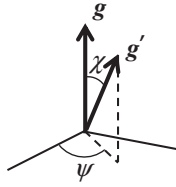


Fig. 4. Definition of scattering angles χ and ψ .³⁸⁾

$$\xi_5 = \int_0^\chi q(\varepsilon, \theta') \sin \theta' d\theta' / \int_0^\pi q(\varepsilon, \theta') \sin \theta' d\theta', \quad (5)$$

$$\psi = 2\pi\xi_6, \quad (6)$$

where $q(\varepsilon, \theta')$ is the differential cross section at the energy ε and angle θ' . When electron scattering is assumed to be isotropic, the scattering angle χ can be calculated as

$$\cos \chi = 1 - 2\xi_5. \quad (7)$$

The speed for relative velocity after collision $|g'|$ is obtained from the principle of the conservation of energy. For elastic collision, the total kinetic energy of colliding molecule and electron is conserved, and $|g'|$ is equal to $|g|$. For inelastic collision, $|g'|$ is calculated as

$$|g'| = \sqrt{|g|^2 - \frac{2}{\mu} \varepsilon_{th}}, \quad (8)$$

where μ is the reduced mass described as $\mu = mM/(m + M)$ and ε_{th} is the threshold energy for the collision. For superelastic collision, which is the inverse process of the excitation collision having the threshold energy ε_{th} , $|g'|$ is calculated as

$$|g'| = \sqrt{|g|^2 + \frac{2}{\mu} \varepsilon_{th}}. \quad (9)$$

The number density N is $3.535 \times 10^{16} \text{ cm}^{-3}$ at 0°C and 1 Torr, and the collision between an electron and a H_2O molecule is only considered, assuming the low ionization degree in a typical swarm experiment. The populations of rotational excitation states for thermally excited molecules are neglected because of a lack of reliable data for rotational excitation.

4. Results and discussion

4.1 Comparison between measured and calculated transport coefficients

Figure 5 shows the values of mean-arrival-time drift velocity W_m in water vapor calculated from the present cross section set as a function of E/N , together with those calculated from the cross section sets reported by Yousfi and Benabdessadok,¹¹⁾ Itikawa and Mason,¹⁰⁾ and de Urquijo et al.¹²⁾ The values of W_m measured by the double-shutter drift tube method³⁴⁾ and pulsed experiment¹²⁾ are also plotted. The calculated values from the Yousfi and Benabdessadok's cross section set¹¹⁾ are close to the measured data below $E/N = 40 \text{ Td}$ and above $E/N = 160 \text{ Td}$, but they do not agree with the measured data between 40 and 160 Td. Although the calculated values from Itikawa and Mason's cross section set¹⁰⁾ disagree with the measured data, the values of W_m calculated from the cross section sets estimated here and reported by de Urquijo et al.¹²⁾ are found to agree well with the measured data.

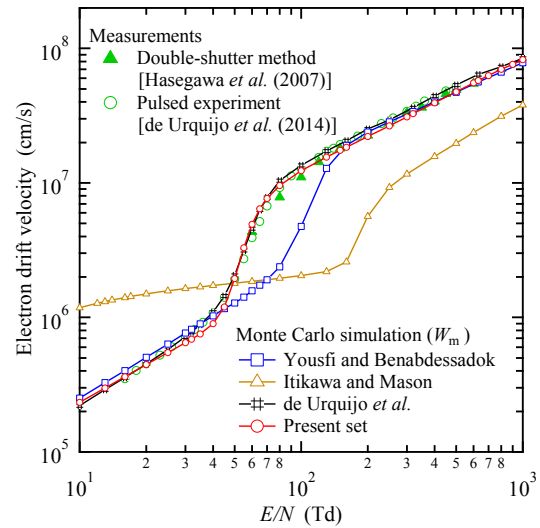


Fig. 5. (Color online) Electron drift velocity in water vapor as a function of E/N .

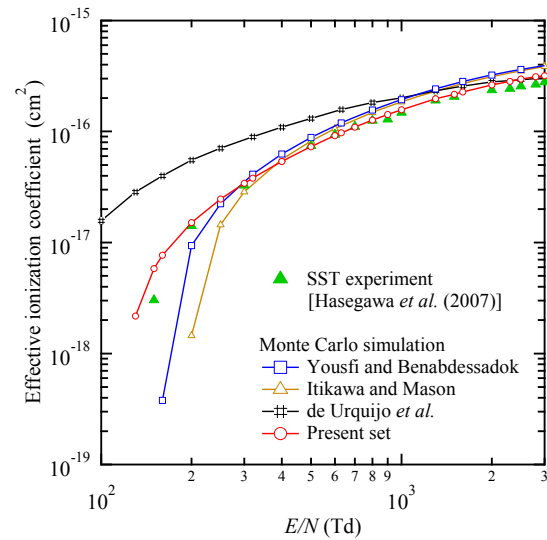


Fig. 6. (Color online) Effective ionization coefficient in water vapor as a function of E/N .

Figure 6 shows the values of effective ionization coefficient $(\alpha - \eta)/N$ in water vapor calculated from the present cross section set as a function of E/N , together with those calculated from the previously reported cross section sets¹⁰⁻¹²⁾ and measured by steady-state Townsend experiment.³⁴⁾ The $(\alpha - \eta)/N$ values calculated from the cross section set reported by de Urquijo et al.¹²⁾ are larger than the measured data in a wide range of E/N values. The values calculated from the other reported cross section sets^{10,11)} are close to the measured data between 300 and 800 Td, but disagree with the measured data in the other E/N region. The values calculated from the present cross section set agree with the measured data within the difference of 10% between 200 and 2,000 Td, and within the difference of 15% above $E/N = 2,000 \text{ Td}$. The difference in $(\alpha - \eta)/N$ above 2,000 Td may affect the ionization growth of electrons. Although the difference between the calculated value and measured data is found to be 48% at $E/N = 150 \text{ Td}$, $(\alpha - \eta)/N$ is quite small; therefore, the influence of the difference in $(\alpha - \eta)/N$ on the ionization growth of electrons can be ignored.

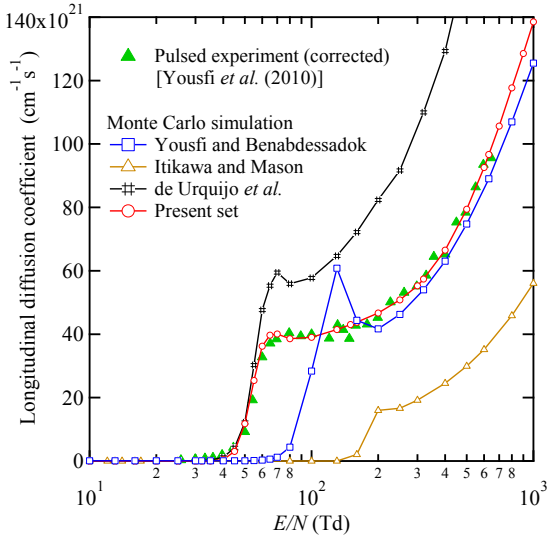


Fig. 7. (Color online) Longitudinal diffusion coefficient in water vapor as a function of E/N .

Figure 7 shows the values of longitudinal diffusion coefficient ND_L in water vapor calculated from the present cross section set as a function of E/N , together with those calculated from the previously reported cross section sets^{10–12} and measured by pulsed experiment.³⁹ Here, the values of ND_L measured by pulsed experiment are corrected in accordance with the relation with ND_L measured by TOF experiment reported by Terashita et al.⁴⁰ The values of ND_L calculated from Yousfi and Benabdessadok's set¹¹ are close to the measured data above $E/N = 200$ Td, but disagree with the data below $E/N = 160$ Td. Those calculated from the other reported cross section sets^{10,12} disagree with the measured data. The ND_L values calculated from the present cross section set agree well with the measured data.

The electron transport coefficients calculated from the present cross section set agree well with the measured data in a wide range of E/N values, and this confirms the validity of the present cross section set.

4.2 Influences of superelastic collision on transport properties

Since superelastic collision for rotationally excited molecules may affect the transport properties of electrons in water vapor, especially at low E/N values, the superelastic collision has been considered in several studies.^{11,12,41} Thus, the influences of the superelastic collision on the electron transport coefficients in water vapor are examined. Figure 8 shows the superelastic collision cross sections $q_{J' \rightarrow 0}$ for the transition from $J = J'$ to 0 calculated from the following equation derived from the principle of detailed balance:³⁶

$$q_{J' \rightarrow 0}(\varepsilon) = \frac{1}{2J' + 1} \frac{\varepsilon + \varepsilon_{th}}{\varepsilon} q_{0 \rightarrow J'}(\varepsilon + \varepsilon_{th}), \quad (10)$$

where $q_{0 \rightarrow J'}$ is the rotational excitation cross section for the transition from $J = 0$ to J' and ε_{th} is the threshold energy of $q_{0 \rightarrow J'}$. The scattering angle after the superelastic collision is calculated using the differential cross sections shown in Fig. 3.

Figure 9 shows the values of W_m , $(\alpha - \eta)/N$, and ND_L calculated from the cross section set considering the super-

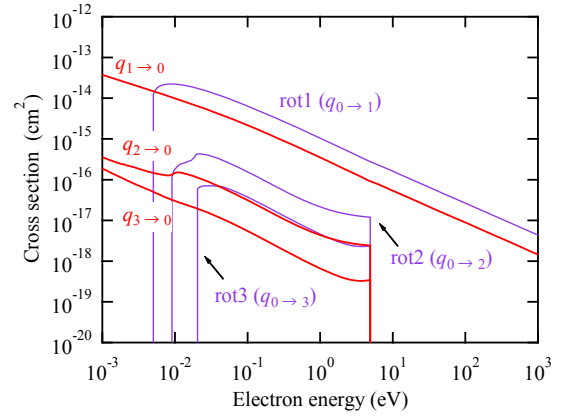
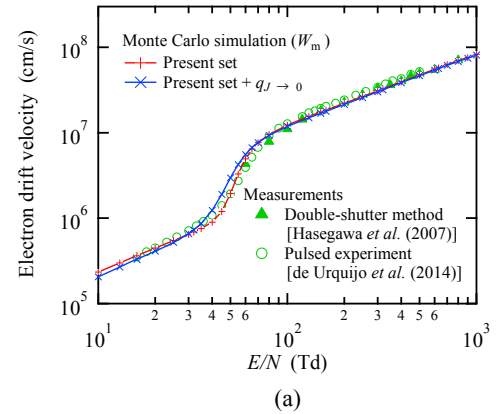
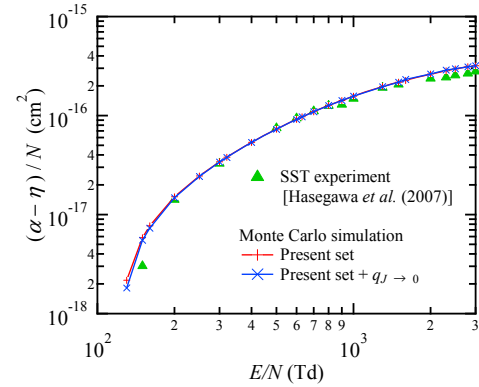


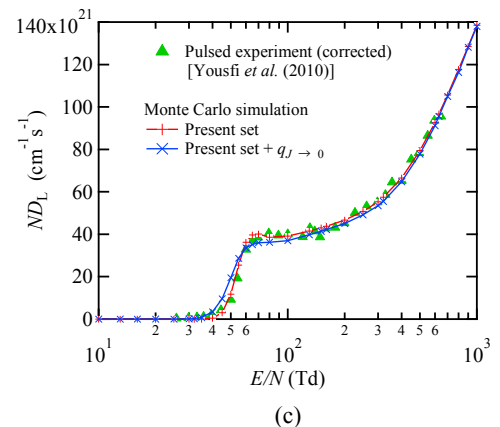
Fig. 8. (Color online) Superelastic collision cross sections for water vapor.



(a)



(b)



(c)

Fig. 9. (Color online) Influence of superelastic collision on the electron transport coefficients in water vapor: (a) electron drift velocity, (b) effective ionization coefficient, and (c) longitudinal diffusion coefficient.

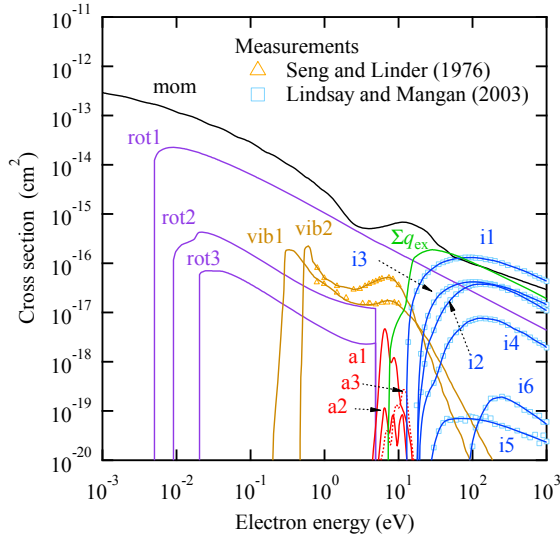


Fig. 10. (Color online) Electron collision cross sections of water vapor assuming the isotropic electron scattering (isotropic scattering model).

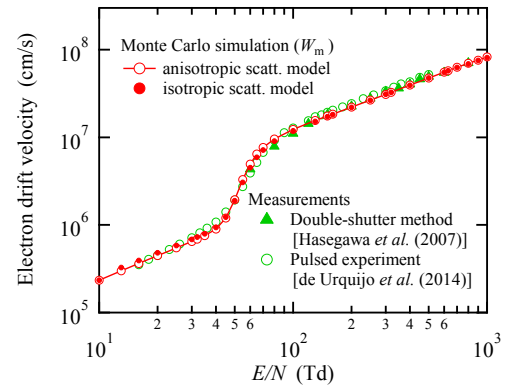
elastic collision as functions of E/N . The slight influence of superelastic collision on W_m and ND_L is found below $E/N = 100 \text{ Td}$, but no significant difference is found in $(\alpha - \eta)/N$. This indicates that the influence of superelastic collision is negligible and limited.

4.3 Isotropic scattering model for practical use

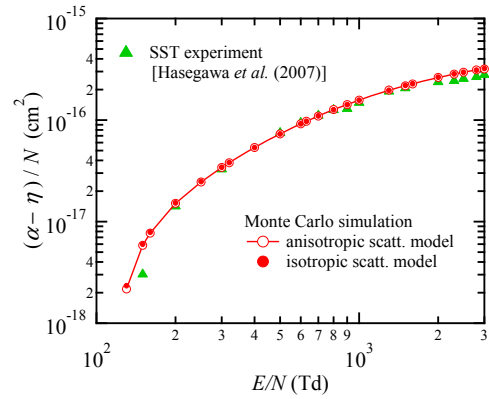
In the calculation of electron transport coefficients and rate coefficients using electron collision cross sections, it is not necessarily easy to consider the anisotropic electron scattering. Moreover, those coefficients are often calculated by a two-term approximation Boltzmann equation solver like BOLSIG+,⁴²⁾ which assumes electron scattering to be isotropic. For practical use, the electron collision cross section set for water vapor assuming the isotropic electron scattering is therefore estimated. Figure 10 shows the estimated cross section set called the isotropic scattering model. The elastic collision cross section in Fig. 1 is replaced with the elastic momentum transfer cross section shown in Fig. 10. The other cross sections are the same as those in Figs. 1 and 2.

Figure 11 shows the values of the electron transport coefficients in water vapor calculated by Monte Carlo simulation using the cross section sets shown in Fig. 1 (anisotropic scattering model) and Fig. 10 (isotropic scattering model) as functions of E/N , together with the measured data.^{12,34,39)} It is found that the transport coefficients calculated from the cross section set assuming the isotropic electron scattering agree with those calculated from the cross section set considering the anisotropic electron scattering.

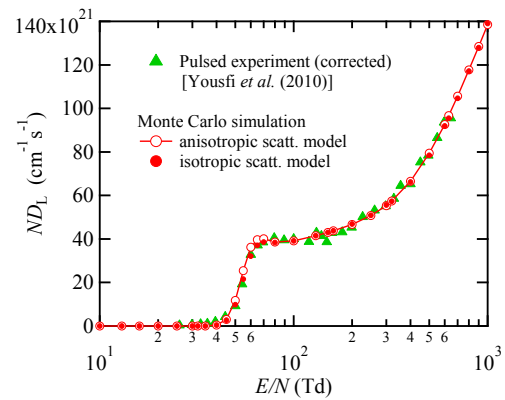
Figures 12 and 13 show rate coefficients such as Σk_{rot} , Σk_{vib} , Σk_a , Σk_{ex} , and Σk_i and those concerning OH radical generation in water vapor calculated from the two cross section sets as functions of E/N , respectively. Symbols Σk_{rot} , Σk_{vib} , Σk_a , Σk_{ex} , and Σk_i in Fig. 12 denote the sum of rate coefficients for rotational excitation, vibrational excitation, electron attachment, electronic excitation, and ionization collisions, respectively. The rate coefficients calculated from the two cross section sets agree very well. This indicates that the cross section set assuming the isotropic electron



(a)



(b)



(c)

Fig. 11. (Color online) Comparison between the electron transport coefficients calculated from the two cross section sets: (a) electron drift velocity, (b) effective ionization coefficient, and (c) longitudinal diffusion coefficient.

scattering can be used for that considering the anisotropic electron scattering.

5. Conclusions

The reliable electron collision cross section set of water vapor is estimated by the electron swarm method using Monte Carlo simulation. The cross section set consists of two vibrational excitations, three electron attachments, 26 electronic excitations, six ionizations, and three rotational excitation cross sections and one elastic collision cross section, and the anisotropic electron scattering for elastic and rotational excitation collisions is considered. The electron

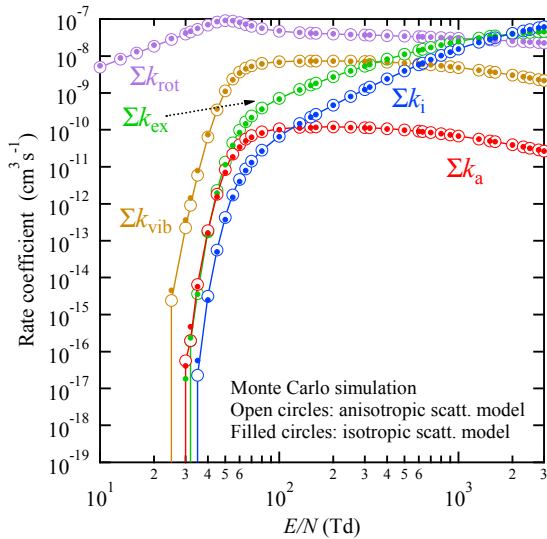


Fig. 12. (Color online) Sum of rate coefficients for inelastic collisions in water vapor.

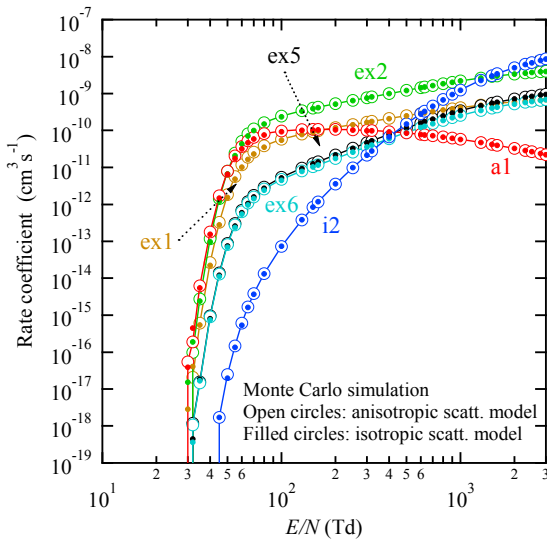


Fig. 13. (Color online) Rate coefficients for the generation of OH radical in water vapor.

transport coefficients calculated from the present cross section set are in good agreement with the measured data in a wide range of E/N values. This confirms the validity of the present cross section set.

The cross section set for water vapor assuming the isotropic electron scattering is proposed for practical use. The electron transport coefficients and rate coefficients calculated by Monte Carlo simulation using the cross section set assuming the isotropic electron scattering are found to agree well with those calculated from the accurate cross section set considering the anisotropic electron scattering.

- 1) J. Takahata, K. Takaki, N. Satta, N. Satta, K. Takahashi, T. Fujio, and Y. Sasaki, *Jpn. J. Appl. Phys.* **54**, 01AG07 (2015).
- 2) C. A. J. van Gils, S. Hofmann, B. K. H. L. Boekema, R. Brandenburg, and

- P. J. Bruggeman, *J. Phys. D* **46**, 175203 (2013).
- 3) H. Kuwahata, T. Yamaguchi, R. Ohya, and A. Ito, *Jpn. J. Appl. Phys.* **54**, 01AG08 (2015).
- 4) E. Usui, T. Ohshima, H. Yamazaki, S. Ikawa, K. Kitano, N. Maeda, and Y. Momoi, *Nihon Shika Hozongaku Zasshi* **58**, 101 (2015) [in Japanese].
- 5) Y. Miyazaki, K. Satoh, and H. Itoh, *Electr. Eng. Jpn.* **174** [2], 1 (2011).
- 6) H. Shiota, H. Itabashi, K. Satoh, and H. Itoh, *Denki Gakkai Ronbunshi A* **132**, 297 (2012) [in Japanese].
- 7) T. Shirafuji and T. Murakami, *Jpn. J. Appl. Phys.* **54**, 01AC03 (2015).
- 8) D. X. Liu, P. Bruggeman, F. Iza, M. Z. Rong, and M. G. Kong, *Plasma Sources Sci. Technol.* **19**, 025018 (2010).
- 9) F. Tochikubo, S. Uchida, and T. Watanabe, *Jpn. J. Appl. Phys.* **43**, 315 (2004).
- 10) Y. Itikawa and N. Mason, *J. Phys. Chem. Ref. Data* **34**, 1 (2005).
- 11) M. Yousfi and M. D. Benabdessadok, *J. Appl. Phys.* **80**, 6619 (1996).
- 12) J. de Urquijo, E. Basurto, A. M. Juárez, K. F. Ness, R. E. Robson, M. J. Brunger, and R. D. White, *J. Chem. Phys.* **141**, 014308 (2014).
- 13) G. Seng and F. Linder, *J. Phys. B* **9**, 2539 (1976).
- 14) P. Rawat, V. S. Prabhudesai, G. Aravind, M. A. Rahman, and E. Krishnakumar, *J. Phys. B* **40**, 4625 (2007).
- 15) C. E. Melton, *J. Chem. Phys.* **57**, 4218 (1972).
- 16) P. A. Thorn, PhD Thesis, School of Chemistry, Physics and Earth Sciences, Flinders University, Adelaide (2008).
- 17) M. J. Brunger, P. A. Thorn, L. Campbell, N. Diakomichalis, H. Kato, H. Kawahara, M. Hoshino, H. Tanaka, and Y.-K. Kim, *Int. J. Mass Spectrom.* **271**, 80 (2008).
- 18) P. A. Thorn, M. J. Brunger, H. Kato, M. Hoshino, and H. Tanaka, *J. Phys. B* **40**, 697 (2007).
- 19) P. A. Thorn, M. J. Brunger, P. J. O. Teubner, N. Diakomichalis, T. Maddern, M. A. Bolorizadeh, W. R. Newell, H. Kato, M. Hoshino, H. Tanaka, H. Cho, and Y.-K. Kim, *J. Chem. Phys.* **126**, 064306 (2007).
- 20) P. Thorn, L. Campbell, and M. Brunger, *PMC Phys. B* **2**, 1 (2009).
- 21) B. G. Lindsay and M. A. Mangan, in *Photon and Electron Interactions with Atoms, Molecules and Ions*, ed. Y. Itikawa (Springer, New York, 2003) Vol. I/17C, Chap. 5.
- 22) H. C. Straub, B. G. Lindsay, K. A. Smith, and R. F. Stebbings, *J. Chem. Phys.* **108**, 109 (1998).
- 23) K. B. Snow and T. F. Thomas, *Int. J. Mass Spectrom. Ion Processes* **96**, 49 (1990).
- 24) D. Lefavre and P. Marmet, *Can. J. Phys.* **56**, 1549 (1978).
- 25) J. D. Morrison and J. C. Traeger, *Int. J. Mass Spectrom. Ion Phys.* **11**, 77 (1973).
- 26) H. Ehrhardt and A. Kresling, *Z. Naturforsch. A* **22**, 2036 (1967) [in German].
- 27) NIST Chemistry Webbook [<http://webbook.nist.gov>].
- 28) A. Faure, J. D. Gorfinkel, and J. Tennyson, *Mon. Not. R. Astron. Soc.* **347**, 323 (2004).
- 29) H. Cho, Y. S. Park, H. Tanaka, and S. J. Buckman, *J. Phys. B* **37**, 625 (2004).
- 30) S. Kawaguchi, K. Satoh, and H. Itoh, *Jpn. J. Appl. Phys.* **54**, 01AC01 (2015).
- 31) S. Kawaguchi, K. Satoh, and H. Itoh, *Eur. Phys. J. D* **68**, 100 (2014).
- 32) Z. Lj. Petrović, S. Dujko, D. Marić, G. Malović, Ž. Nikitović, O. Šašić, J. Jovanović, V. Stojanović, and M. Radmilović-Radenović, *J. Phys. D* **42**, 194002 (2009).
- 33) K. Kondo and H. Tagashira, *J. Phys. D* **23**, 1175 (1990).
- 34) H. Hasegawa, H. Date, and M. Shimozuma, *J. Phys. D* **40**, 2495 (2007).
- 35) K. Satoh, M. Hataguchi, H. Itoh, Y. Sakai, and H. Tagashira, *J. Phys. D* **27**, 1480 (1994).
- 36) M. Yousfi, A. Hennad, and A. Alkaa, *Phys. Rev. E* **49**, 3264 (1994).
- 37) W. H. Press, S. A. Teukolsky, W. T. Vetterling, and B. P. Flannery, *Numerical Recipes* (Cambridge University Press, Cambridge, U.K., 2007) 3rd ed., p. 364.
- 38) R. E. Robson, *Introductory Transport Theory for Charged Particles in Gases* (World Scientific, Singapore, 2006) p. 26.
- 39) M. Yousfi, J. de Urquijo, A. Bekstein, E. Basurto, O. Eichwald, J. L. Hernández-Ávila, M. Benhenni, A. M. Juárez Reyes, and N. Merbahi, *Proc. 17th Int. Conf. Gas Discharges and Their Applications*, 2010, p. 574.
- 40) Y. Terashita, K. Satoh, and H. Itoh, *Denki Gakkai Ronbunshi A* **134**, 454 (2014) [in Japanese].
- 41) K. F. Ness and R. E. Robson, *Phys. Rev. A* **38**, 1446 (1988).
- 42) G. J. M. Hagelaar and L. C. Pitchford, *Plasma Sources Sci. Technol.* **14**, 722 (2005).